Detection Algorithm of a Heat-transfer System Based on Pennes Bio-heat Transfer Formula Processing

Wenju Ji[1,*], Jianwen Wang[2]

[1]*Inner Mongolia University of Technology*
Hohhot, Inner Mongolia 010051, China
E-mail: jiwenjujwj@163.com

[2]*Wind and Solar Energy Utilization Technology Key Laboratory*
Provincial Department of the Ministry of Education
Inner Mongolia University of Technology
Hohhot, Inner Mongolia 010051, China
E-mail: wangjianwenwjww@sina.com

[*]*Corresponding author*

Received: November 09, 2015 **Accepted: June 1, 2016**

Published: June 30, 2016

Abstract: *Biological experiments and clinical trials indicate that low temperature treatment technology is of great significance to the treatment of craniocerebral injury by protecting the brain nerves and reducing its sequela. However, the major challenge at present is how to appropriately control the degree and timing sequence of hypothermia in treating craniocerebral injury in order to meet the requirement of protecting the brain and reducing the side effects. By establishing a mathematical model of craniocerebral heat transfer, this paper theoretically studies the forecast of temperature distribution of the brain and the selective refrigeration control. Furthermore, this study provides guidance for practical clinical treatment by researching the rules of hypothermia and warming in different parts of the brain.*

Keywords: *Craniocerebral injury, Low temperature therapy, Temperature distribution, Selective refrigeration, Parameter estimation.*

Introduction

One of the important factors that cause a patient's death in craniocerebral injury treatment is cerebral lesion, including ischemia, unsmooth blood flow, regional hypoxia and overheating [12]. In China, with its high disability rate, brain injury has become a leading lethal factor among young adults [8].

The Pennes model is a classical model to describe the heat transfer process in biological tissue. Due to its simple form, the Pennes model is still the most widely applied biological heat transfer model; there have been clinical applications of the Pennes model in tumor thermotherapy [1], burn [2] and low temperature operation [14]. In 1948, Pennes published a theoretical research report on heat transfer in a human forearm, which laid foundation for biological heat transfer theory. Based on the Pennes model, some scholars researched on heat transfer by improving and establishing models. Jiang et al. [7] established a mathematical model to describe scalding of skin tissue by hot water; they analyzed the law of the heat transfer process and predicted the scalding degree. Zeng et al. [13] proposed a numerical solution to the three-dimensional Pennes equation with the particular solution boundary element method. Zhang et al. [15] gave a numerical solution to the equation with the finite element and finite difference method.

From the perspective of mathematics and engineering, the present study analyzes cerebral low-temperature control and proposes methods to treat craniocerebral injury. Thereby, based on the control theory, we put forward the theoretical methods of craniocerebral low-temperature control as well as a regulating mechanism of craniocerebral temperature distribution in order to provide theoretical foundations for the development of actual control devices and clinical experiments.

Material and methods

First, we established a mathematical model regarding temperature distribution and changes in the process of selective craniocerebral refrigeration. Then, based on the model and its solving method, we performed a steady-state analysis and a dynamic analysis on the temperature characteristics of the craniocerebral mathematical model and predicted the temperature distribution curve during hypothermia treatment. Afterwards, we explored theoretically the temperature distribution of the simulated brain and discussed the changing tendency of brain temperature over time and the effect of each parameter on the temperature distribution with selective brain refrigeration [3]. Based on the above methods, the dynamic characteristics of the craniocerebral mathematical model were approximated to first order process objects. According to the control theory, control parameters were obtained through system identification of first-order process objects. By substituting the parameter into a proportional-integral-derivative (PID) controller, the whole hypothermia and warming process of craniocerebral selective refrigeration could be controlled.

Results and discussion

Mathematical modeling of craniocerebral heat transfer process

Heat-transfer model of craniocerebral cryogenic treatment

Based on the craniocerebral structure, blood circulation and heat-transfer characteristics, we simplified the structure of different parts of the brain and applied the Pennes bio-heat transfer equation [5, 6]. As the brain shape is similar to a hemisphere, we adopted a hemispherical heat transfer model for mathematical modeling of brain hypothermia treatment [9]. The bottom of the hemisphere was considered to be dynamic and adiabatic since temperature distribution and cerebral changing were the research objects.

As shown in Fig. 1, all layers conformed to the features of biological heat transfer. Accordingly, the Pennes bio-heat transfer equation was applied in the modeling of each layer.

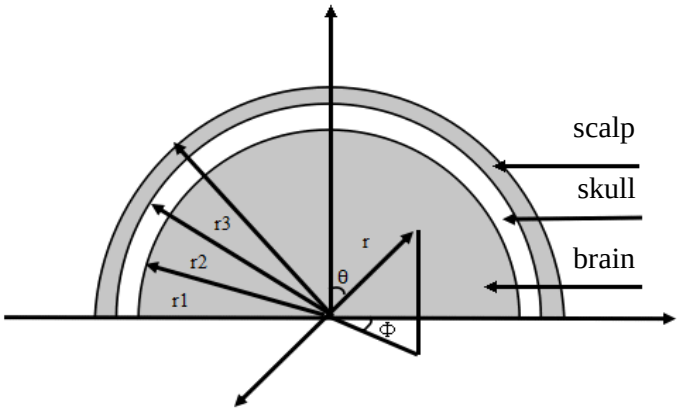

Fig. 1 Hierarchical diagram of head modeling

The following equations were respectively the heat transfer equations of mathematical models of head, skull and hair:

$$\text{Brain: } (\rho c_p)_{brain}\frac{\partial T}{\partial t} = k_{brain}\Delta T + (\rho c_p)_b w_{brain}(T_a - T) + q_{brain}, \quad (1)$$

$$\text{Skull: } (\rho c_p)_{skull}\frac{\partial T}{\partial t} = k_{skull}\Delta T + (\rho c_p)_b w_{skull}(T_a - T) + q_{skull}, \quad (2)$$

$$\text{Hair: } (\rho c_p)_{scalp}\frac{\partial T}{\partial t} = k_{scalp}\Delta T + (\rho c_p)_b w_{scalp}(T_a - T) + q_{scalp}. \quad (3)$$

Considering the thermal continuity between different layers and the adiabaticity of the hemisphere model bottom, the following boundary conditions were also required:

$$\text{Adiabaticity: } \frac{\partial T}{\partial r} = 0,\ (if)\, r = 0, \quad (4)$$

$$\text{Continuity: } \begin{matrix} \frac{\partial T_{brain}}{\partial r} = \frac{\partial T_{skull}}{\partial r},\ (if)\, r = r_1 \\ \frac{\partial T_{skull}}{\partial r} = \frac{\partial T_{skull}}{\partial r},\ (if)\, r = r_2 \end{matrix}, \quad (5)$$

$$\text{Boundary: } T_{scalp} = T_{skin},\ (if)\, r = r_3. \quad (6)$$

Eqs. (1)-(3) and boundary conditions (4)-(6) were used to simplify and establish a mathematical model for the craniocerebral treatment at low temperature. All equations were solved under spherical coordinates. Considering the symmetry of a sphere, some of the Laplace operators in this study can be simplified, as shown in Eq. (7):

$$\Delta T = \frac{1}{r^2}\frac{\partial}{\partial}\left(r^2\frac{\partial T}{\partial r}\right). \quad (7)$$

Based on the equations above, the temperature field distribution and the temperature change characteristic of the cerebral cryogenic treatment model were obtained.

Solution of cerebral cryogenic treatment mathematical model

As a commonly used method to solve partial differential equations, the finite element method (used in this study) can solve equations by variational method to reduce the error [11]. As to the Pennes bio-heat transfer equation in spherical coordinates, each layer can be simplified as follows:

$$\frac{\partial T}{\partial t} = \alpha\frac{1}{r^2}\frac{\partial}{\partial r}\left(r^2\frac{\partial T}{\partial r}\right) - WT + Q. \quad (8)$$

Respectively, $\alpha = \frac{k}{(\rho c)_t}$, $W = \frac{(\rho c)_b}{(\rho c)_t} w_t$, $Q = q_t + \frac{(\rho c)_b}{(\rho c)_t} w_t T$, subscript t means tissue. A random smooth function $\eta(r)$ was selected from boundary Ω and Eq. (8) was multiplied with $\eta(r)$:

$$\int_{R_1}^{R_2} \frac{\partial T}{\partial t} \eta(r) r dr = \int_{R_1}^{R_2} \left(\alpha \frac{1}{r^2} \frac{\partial}{\partial r} \left(r^2 \frac{\partial T}{\partial r} \right) - WT + Q \right) \eta(r) r dr . \tag{9}$$

R_1 and R_2 respectively refer to two radiuses of the boundary. Eq. (9) was simplified with the integration by parts method, and the following equation was obtained:

$$\int_{R_1}^{R_2} \alpha \frac{1}{r^2} \frac{\partial}{\partial r} \left(r^2 \frac{\partial T}{\partial r} \right) \eta(r) r dr = \alpha \left(\frac{\partial T}{\partial t} \eta(r) \Big|_{R_1}^{R_2} \right) - \alpha \int_{R_1}^{R_2} \left(r\eta(r) - \eta(r) \right) \frac{\partial T}{\partial t} dr . \tag{10}$$

The interval [R_1, R_2] was divided into N sub-intervals. The temperature function was defined as follows:

$$T^N(r,t) = \sum_{i=0}^{N} X_i(t) \varphi_i(r) . \tag{11}$$

$\varphi_i(r) = S\left(Nr - i(R_2 - R_1)\right)$, $S(r)$ refers to a first order spline function, which can be written as:

$$S(r) = \begin{cases} R_2 - R_1 + r, \; r \in [R_1 - R_2, \; 0] \\ R_2 - R_1 - r, \; r \in [0, \; R_2 - R_1] \\ 0, \text{ else} \end{cases} . \tag{12}$$

Thus time can be separated from space. Eqs. (10) and (11) were substituted into Eq. (9), and Eq. (13) was obtained:

$$\begin{aligned} &\sum_{i=0}^{N} X_i(t) \int_{R_1}^{R_2} \varphi_i(r) \eta(r) r dr = \alpha \sum_{i=0}^{N} X_i(t) \left(\varphi_i(r) \eta(r) \Big|_{R_1}^{R_2} \right) - \\ &-\alpha \sum_{i=0}^{N} X_i(t) \int_{R_1}^{R_2} \left[\left(r\eta(r) - \eta(r) \right) \right] \varphi(r) - W \sum_{i=0}^{N} X_i(t) \int_{R_1}^{R_2} \varphi_i(r) \eta(r) r dr + Q \int_{R_1}^{R_2} \eta(r) r dr . \end{aligned} \tag{13}$$

Since $\varphi_i(r)$ is known, $\eta(r)$ is a random function in [R_1, R_2]. In the solving process of finite elements, $\eta(r)$ was divided into N sub-intervals. Therefore, the coefficients of $X_i(t)$ in Eq. (13) were constants. Suppose:

$$X = \left[X_0(t) \quad X_1(t) \cdots X_N(t) \right],$$

$$A = \int_{R_1}^{R_2} \varphi_i(r) \eta(r) r dr,$$

$$B = \left(\varphi_i(r) \eta(r) \Big|_{R_1}^{R_2} \right) - \int_{R_1}^{R_2} \left[\left(r\eta(r) - \eta(r) \right) \right] \varphi(r),$$

$$C = \int_{R_1}^{R_2} \eta(r) r dr.$$

Then, Eq. (13) can be simplified as:

$$AX = \alpha BX - WAX + C. \tag{14}$$

Based on an approximate approach with the variational method, partial differential equations were approximated into an ordinary differential equation. At the same time, the approximation degree could be adjusted by adjusting the partition amount: the more partition, the closer to the authentic solution [5, 10]. As for ordinary differential equations similar to Eq. (14), as long as their initial conditions were obtained, the equations could be solved by numerical solution of ordinary differential equations, for example, the Runge Kutta method.

According to the mathematical derivation above, through segmentation and variation with the finite element method, the numerical solution of the three-level craniocerebral refrigeration mathematical model could be obtained, which laid the basis for further analysis.

Characteristics of the temperature distribution of the selective craniocerebral refrigeration model

Basic characteristics of the temperature distribution of the model

Under normal circumstances, there is a heat transfer between the scalp and the environment. Assuming that the environmental temperature T_{air} = 20 °C, according to the Newton's law of cooling, the boundary condition (Eq. (6)) was rewritten as:

$$\frac{\partial T}{\partial t} = h\left(T - T_{air}\right). \tag{15}$$

In Eq. (15), the air heat exchange coefficient $h = h_{air}\left(L, P_a, T_{air}\right)$, L is diameter and P_a is atmospheric pressure, which can be calculated, based on the current temperature and air pressure. In this study, we adopted the standard atmospheric pressure and ambient temperature. According to the heat transfer theory, the boundary condition (Eq. (6)) of the mathematical model was changed into the boundary condition (Eq. (15)). The steady-state temperature distribution curve of the craniocerebral brain under normal conditions was obtained by solving the model. As shown in Fig. 2, the temperature distribution from the inside to the outside ranged from 37.3 °C to 36.0 °C. The radius of the brain was 85 mm; at 70 mm of the radius, the temperature reduced to 36.7 °C from 37.3 °C. The gray layer was located at 67 mm to 85 mm of the radius. According to the data, it can be observed that under normal circumstances, the temperature of the gray layer reduced from the inside to the outside, while the temperature of the white matter layer (within 67 mm of the radius) remained 37.3 °C.

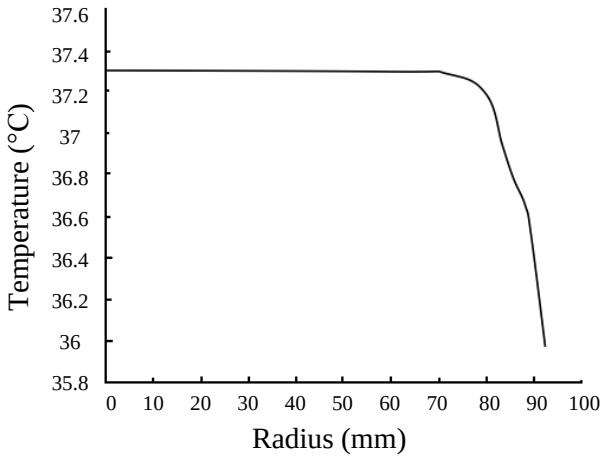

Fig. 2 Steady-state temperature distribution curve of the craniocerebral brain under normal conditions

In this study, selective craniocerebral refrigeration was achieved by cooling the scalp. The external controllable cooling device was worn on the head directly, which kept the scalp at the boundary temperature (T_{skin}) and finally reduced the temperature through heat transfer. In this study, specific heat, thermal conductivity, blood perfusion rate and other parameters were the statistical results of clinical studies (as shown in Table 1).

Table 1. Tissue parameters of each part

Tissue	Brain	Skull	Scalp	Blood
Specific heat (W/kg.K)	3700	2300	4000	3800
Density (kg/m^3)	1050	1500	1000	1050
Thermal conductivity (W/m.K)	0.60	1.12	0.33	-
Blood perfusion rate (1/s)	0.00876	0.00032	0.00030	-
Metabolic rate (K/m^3)	10436	368.2	363.5	-
Radius (Adult) (mm)	84	88	92	-

Note: The parameters in Table 1 are taken from document statistics [6].

Selective craniocerebral refrigeration control

Adjusting of temperature control parameters of craniocerebral cryogenic refrigeration

Based on process object identification, the first order object model can be used to approximate the values of the process model of the bio-heat transfer equation model [4]. Temperature control of the measurement point could be achieved by controller parameter setting of the first order object model on Simulink. Meanwhile, according to the actual parameter requirement, the bio-heat transfer model was used directly. The controller used in this study was PID whose controlling expression is shown as formula (16):

$$T_{skin} = P\left(T_{set} - T\right) + I\int_0^l \left(T_{set} - T\right)dt + D\frac{d(T_{set} - T)}{dt}. \quad (16)$$

Considering that the parameter needs to be re-adjusted after the first setting, we only needed to determine the approximate parameters. In the study, we adopted the critical ratio method for its simple and rapid operation. Its PID controller expression is shown as follows:

$$T_{skin} = K_c\left[\left(T_{set} - T\right) + \frac{1}{T_i}\int_0^l \left(T_{set} - T\right)dt + T_d\frac{d\left(T_{set} - T\right)}{dt}\right] \quad (17)$$

Therefore, $P = K_c$, $I = \frac{K_c}{T_i}$, $D = K_c T_d$. From Fig. 3 it can be obtained that the relevant parameter P_u = 2.6 min and the controller gain K_{cmax} = 21. According to Table 2, the PI controller parameter was adjusted to better reduce the craniocerebral temperature in accordance with the existing setting (P = 9.4, I = 4.37). After repeated adjustment, preferable PI controller coefficients were obtained: P = 0.8, I = 2, D = 0.

Table 2. The control law of the critical ratio method

Control law	P	PI	PID
K_c	$0.5K_{cmax}$	$0.45K_{cmax}$	$0.6K_{cmax}$
T_i	-	$0.83P_u$	$0.5P_u$
T_d	-	-	$0.12P_u$

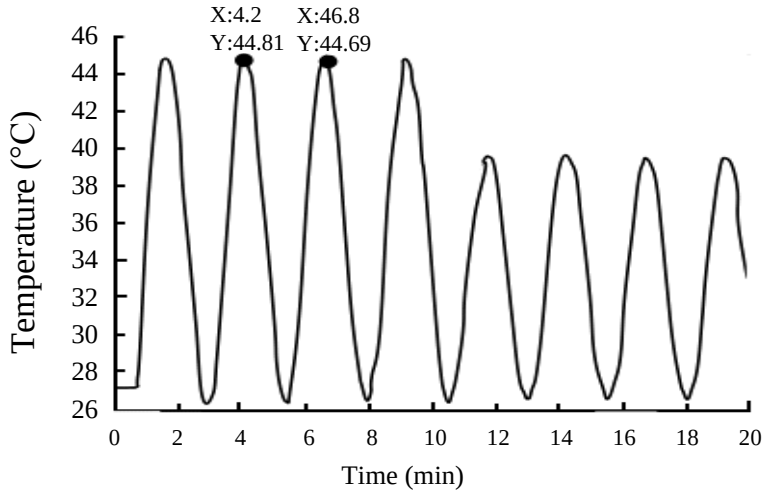

Fig. 3 Schematic graph of continuous oscillation

Cooling and warming settings of selective craniocerebral refrigeration

In the process of craniocerebral refrigeration, the temperature range had a certain influence on its physiological parameter index. So, for hypothermia, not only should brain temperature be in the range of mild hypothermia, but also it should strictly control the cooling depth and its duration, which can help to avoid complications and other tissues coagulation. Therefore, the whole process needs to be set carefully. That is to say, good cooling strategies can achieve the best therapeutic effect.

In this study, the cooling time was set as 7 hours. During the first two hours, the temperature was reduced from 37 °C to 35 °C at the speed of 1 °C/h. After that, the temperature remained 35 °C for two hours, which let the human body fully adapt to the cooling process. For the last three hours, the temperature was set to be 32 °C from 35 °C at the same cooling speed (1 °C/h). Since then, the temperature remained 32 °C, which was the proper temperature for surgeries. Once the surgery was completed, patients needed heating treatment. Fig. 4 shows the temperature settings for selective craniocerebral refrigeration control.

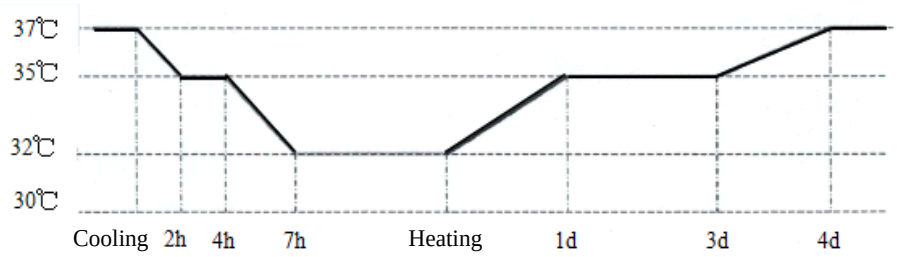

Fig. 4 Temperature settings for selective craniocerebral refrigeration control

Results of selective craniocerebral refrigeration control

Based on the PI control parameters and temperature settings, the scalp temperature was controlled with the PI controller so that the craniocerebral refrigeration curve conformed to the set curve for cooling and heating in order to ensure the treatment effect.

As can be seen from Fig. 5, with the set cooling curve, the selective craniocerebral cooling control could achieve a satisfactory effect for craniocerebral cooling in the bio-heat transfer model. In addition, the cooling curve was changing according to the set process, and the controller precisely controlled the temperature in the process of craniocerebral refrigeration.

Fig. 6 shows the changes of the input control temperature of the scalp and the output temperature of specific points of the brain in the cooling process. As can be seen from the input temperature, the surface temperature of the scalp reduced to 17 °C (the minimum required temperature) from 35 °C (the required temperature to maintain balance). In the whole process, the scalp surface temperature was no less than 15 °C. Therefore, during craniocerebral refrigeration control of the scalp surface, brain temperature could be reduced to mild hypothermia according to the setting curve, without using extra low temperature. Accordingly, we can deduce that in the last chapter, the settings for cooling time and cooling speed were reasonable.

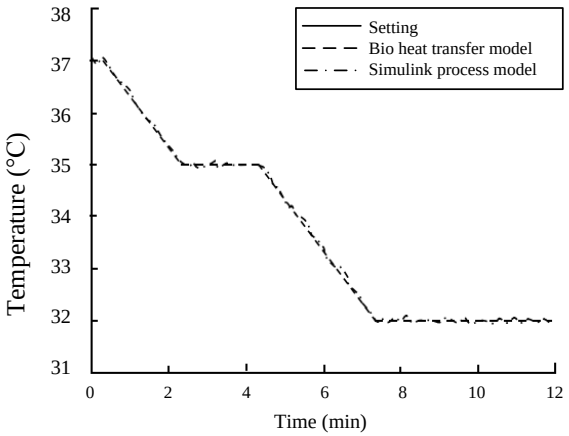

Fig. 5 Temperature curve of the cryogenic cooling process of the craniocerebral brain

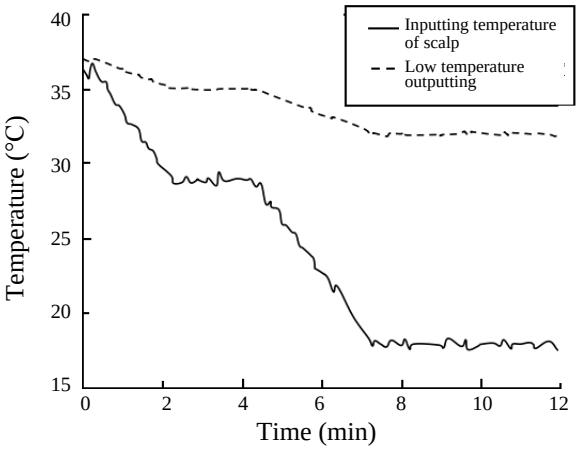

Fig. 6 Input and output curves of the cooling process under the control of mild hypothermia

Fig. 7 shows the temperature curve of selective craniocerebral temperature control in a heating process, from which it can be seen that the output of temperature control curve was basically consistent with the setting curve. In the heating process, the temperature controller could adjust the efficiency and stability of the cooling process. Considering that the heating process was

slow and the controller could adjust the temperature, the heating process was more stable than the cooling process.

Fig. 8 shows the input control temperature of the scalp and the output temperature of specific points of the brain in the heating process. The input temperature gradually increased from constant 17 °C (in a mild hypothermia state) and reached 28 °C when the craniocerebral output temperature was 35 °C. With the gradual increasing of the input temperature, the internal temperature of craniocerebral brain increased to 37 °C. During the whole process, the input temperature increased gradually and finally remained 35 °C.

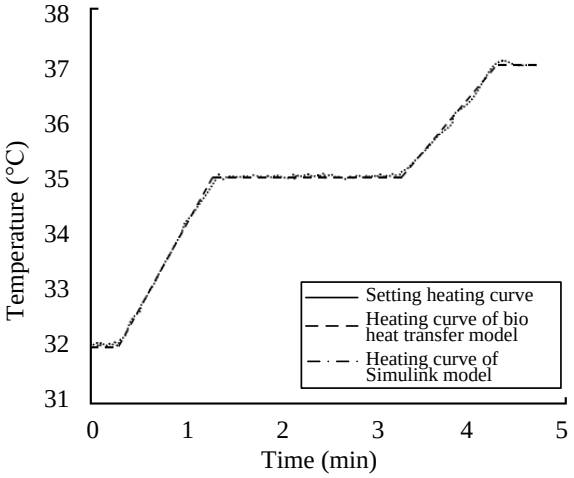

Fig. 7 Heating curve of craniocerebral temperature control

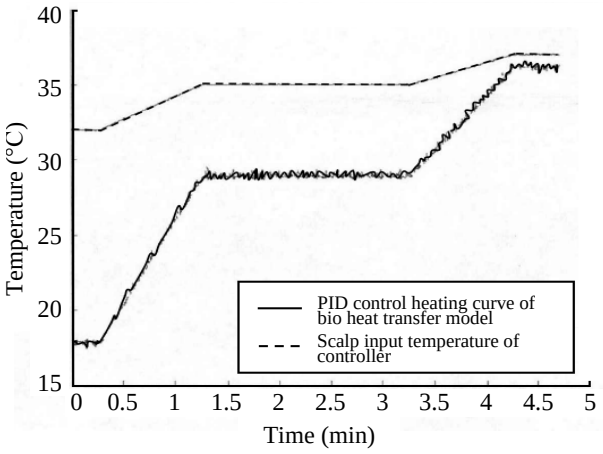

Fig. 8 Input and output curves of the heating process

Conclusion

From the perspective of theoretical research, this study systematically performed refrigeration control based on a craniocerebral model; with a static or a dynamic craniocerebral refrigeration model, parameter estimation could be realized, and models could be modified so as to provide guidance for practice. Craniocerebral refrigeration is an important research direction; this study is not comprehensive yet, accordingly, there will be further studies on craniocerebral refrigeration.

References

1. Alamiri A. M. (2013). Fluid-structure Interaction Analysis of Pulsatile Blood Flow and Heat Transfer in Living Tissues during Thermal Therapy, Journal of Fluids Engineering, 135(4), 77-82.
2. Chen Y., Y. X. Niu, F. Tang, H. Yang, C. Zhang, N. Jiang, H. L. Yang (2008). Numerical Simulation and Experimental Study on Thermal Damage in *in vitro* Human Skin-tissue by High-intensity Laser, Laser & Infrared, 38(4), 375-378.
3. Cui Z. J., G. D. Chen, R. Zhang (2014). Analytical Solution for the Time-fractional Pennes Bioheat Transfer Equation on Skin Tissue, Advanced Materials Research, 1049-1050, 1471-1474.
4. Diao C. G., L. Zhu, H. Wang (2003). Cooling and Rewarming for Brain Ischemia or Injury: Theoretical Analysis, Ann Biomed Eng, 31(3), 346-353.
5. Hartemink K. J., W. Wisselink, J. A. Rauwerda, A. R. Girbes, K. H. Polderman (2004). Novel Applications of Therapeutic Hypothermia: Report of Three Cases, Critical Care, 8(5), 343-346.
6. Jankowska M. A. (2013). Interval Finite Difference Method for Solving the Problem of

Bioheat Transfer Between Blood Vessel and Tissue, In: Parallel Processing and Applied Mathematics, Lecture Notes in Computer Science, 8385, 644-655.
7. Jiang S. C., M. A. Ning, S. S. Wang, X. X. Zhang (2003). Analysis of Skin Heat Transfer and Prediction of Skin Burn Subjected to a Hot Water Film, Space Medicine & Medical Engineering, 16(6), 400-404.
8. John B., H. W. Allen (2003). The Epidemiology of Traumatic Brain Injury: A Review, Epilepsia, 44(10), 2-10.
9. Lakhssassi A., E. Kengne, H. Semmaoui (2010). Investigation of Nonlinear Temperature Distribution in Biological Tissues by Using Bioheat Transfer Equation of Pennes' Type, Natural Science, 2(3), 131-138.
10. Nakayama A., F. Kuwahara, A. Nakayama (2008). WITHDRAWN: A General Bioheat Transfer Model Based on the Theory of Porous Media, International Journal of Heat & Mass Transfer, 51(11-12), 3190-3199.
11. Poor H. Z., H. Moosavi, A. Morad (2015). Analysis of the DPL Bio-heat Transfer Equation with Constant and Time-dependent Heat Flux Conditions on Skin Surface, Thermal Science, doi: 10.2298/TSCI140128057Z.
12. Xiao H., M. Cheng, J. R. Huang, X. Hu, Y. Xu, K. Liu (2013). Clinical Analysis of 35 Cases of Craniocerebral Injury Patients with Intracranial Infection, Chongqing Medicine, 42(21), 2458-2460.
13. Zeng S., Z. Liang, Y. Shi, J. Wang, Y. J. Guo (2009). Numerical Solution of the Three-dimensional Time-dependent Schroedinger Equation and Its Application, Acta Physica Sinica, 58(12), 8180-8187.
14. Zhang X. M., H. Liang, D. Cui, H. J. Jia, et al (2010). Numerical Simulation Study on Damage Mechanism of Throat Armor, Advanced Materials Research, 148-149, 289-292.
15. Zhang Y. M., R. Jing, R. Xiao, Q. Zhang, Y. S. Huang (2013). Comparative Study of 1,064-nm Laser-induced Skin Burn and Thermal Skin Burn, Cell Biochemistry & Biophysics, 67(3), 1005-1014.

Wenju Ji
E-mail: jiwenjujwj@163.com

Wenju Ji was born in Inner Mongolia in April, 1978. Now he is a senior engineer in Inner Mongolia University of Technology.

Jianwen Wang
E-mail: wangjianwenwjww@sina.com

Jianwen Wang was born in Inner Mongolia and now he works in Wind and Solar Energy Utilization Technology Key Laboratory at Provincial Department of the Ministry of Education.